



ELSEVIER

Journal of Membrane Science 135 (1997) 237–243

---

---

**Journal of  
MEMBRANE  
SCIENCE**

---

---

## Sol–gel synthesis of molecular sieving silica membranes

Balagopal N. Nair<sup>a,\*</sup>, Takeo Yamaguchi<sup>c</sup>, Tatsuya Okubo<sup>c</sup>, Hideo Suematsu<sup>a</sup>,  
Klaas Keizer<sup>b</sup>, Shin-Ichi Nakao<sup>c</sup>

<sup>a</sup> Japan High Polymer Center, 2-22-13 Yanagibashi, Taito-ku, Tokyo 111, Japan

<sup>b</sup> VITO, Boeretang 200, B-2400 Mol, Belgium

<sup>c</sup> Department of Chemical System Engineering, University of Tokyo, 7-3-1 Hongo, Bunkyo-ku, Tokyo 113, Japan

Received 4 March 1997; received in revised form 27 May 1997; accepted 28 May 1997

---

### Abstract

Polymeric silica sol was synthesized by the acid catalyzed hydrolysis and condensation of tetra-ethyl-ortho-silicate. Calcined unsupported membranes made from this sol showed microporous nature. Supported membranes on alumina were prepared by dipping and calcining. Helium showed activated diffusion with an apparent activation energy of 17 kJ mol<sup>-1</sup>. H<sub>2</sub> permeation was comparable to that of helium under identical conditions. N<sub>2</sub>, Ar, O<sub>2</sub>, C<sub>3</sub>H<sub>6</sub>, C<sub>3</sub>H<sub>8</sub>, *n*-C<sub>4</sub>H<sub>10</sub> and *i*-C<sub>4</sub>H<sub>10</sub> permeation values were extremely small and therefore difficult to fit appropriate diffusion models. At 303 K hydrocarbon permeation was about 2 times higher than that of N<sub>2</sub>, Ar or O<sub>2</sub>. He/N<sub>2</sub> permselectivity around 1000 and helium permeation in the order of 10<sup>-7</sup>–10<sup>-8</sup> mol m<sup>-2</sup> s<sup>-1</sup> Pa<sup>-1</sup> were measured in the temperature range of 303–460 K. Comparison of *E*<sub>act</sub>, selectivity and He and N<sub>2</sub> permeation of different samples evidenced the dependence of nitrogen flux on processing defects. Obviously permeation rate of nitrogen molecule was insignificant through majority pores of the membrane.

**Keywords:** Ceramic membranes; Microporous membranes; Gas separations

---

### 1. Introduction

Sol–gel silica membranes possess extremely small pore sizes. Membranes with pore sizes in the range of 5–8 Å are commonly made [1–3]. Such membranes have been shown to exhibit activated diffusion, with apparent activation energies (*E*<sub>act</sub>) around 10 kJ mol<sup>-1</sup> for small gas molecules such as He or H<sub>2</sub> [4,5]. The permeation rates through these membranes were in the range of 10<sup>-7</sup>–10<sup>-8</sup> mol m<sup>-2</sup> s<sup>-1</sup> Pa<sup>-1</sup>. However separation factors were limited to the range of 10–20 for gas combinations such as He/N<sub>2</sub>. These values

were considerably smaller than those of CVD silica membranes.

Tsapatsis and Gavalas [6] has made silica membranes with high selectivity and permeability by a CVD process. H<sub>2</sub>/N<sub>2</sub> selectivity as high as 750 was reported at 600°C with a H<sub>2</sub> permeation of 10<sup>-8</sup> mol m<sup>-2</sup> s<sup>-1</sup> Pa<sup>-1</sup>. Yan et al. [7] made CVD membranes with higher selectivity and permeability. Selectivity above 1000 was available at 600°C. Wu et al. [8] reported He/N<sub>2</sub> selectivity of 513 at nearly the same conditions. The activation energies for helium of these membranes were between 5 and 17.3 kJ mol<sup>-1</sup>. The membranes with maximum selectivity showed the highest helium activation energy but non-activated N<sub>2</sub>

---

\*Corresponding author. Fax: 81-3-5822-7220

permeation. A pore size distribution capable of sieving molecules bigger than  $N_2$  was claimed to be responsible.

Compared to CVD, sol–gel synthesis is easy to perform. Hence, highly selective sol–gel membranes may be more interesting materials for industrial gas separation applications. Synthesis of extremely small pore size membranes, with defect free structure, by sol–gel process was therefore attempted.

It is known that porosity of unsupported silica membranes can be tailor made by controlling the synthesis parameters [9,10]. Such a synthesis of silica polymers involves the hydrolysis and condensation of alkoxides, for example, tetra-ethyl-ortho-silicate (TEOS). Acid catalysis of the reaction will lead to weakly branched polymers [11]. By controlling the amount of catalyst or water, the structure of the polymer can be changed from linear to highly branched. The morphology of the resulting dried membrane depends on the structure of these polymers and their efficiency of packing [12]. The control of the structure of the microporous gel is hence not a difficult task.

Nevertheless the uncertainty in engineering defect-free supported membrane is still a major problem. de Lange et al. [13] had qualified silica membranes in terms of apparent activation energy for hydrogen permeation.  $E_{act}$  values varied between 3.2 and 14.9  $\text{kJ mol}^{-1}$  in his silica membranes. Reasonably high values of  $E_{act}$  for  $N_2$  and  $O_2$  were observed on some of the membranes. Horvath–Kawazoe (H–K) analysis of the  $N_2$  adsorption isotherm of the silica gel showed a bi-modal pore size distribution. The effects of bi-modal pore size distribution on gas permeation, however, is difficult to separate from that of defects.

Defects can be formed during dipping and drying or subsequent calcination stages. The pore size distribution of the support, shrinkage of the thin layer and the interaction between the support and the thin layer are all deciding factors. Moaddeb and Koros [14] had detailed the effects of size and distribution of support pores on the final permeation behavior of polymer layers coated on them. They have shown that the use of large pore size supports could create consistency problems. The relative sizes of the polymer and the pore size of the support is important in this respect. According to them, when the hydrodynamic diameter

of the polymer is larger or of the same magnitude as the diameter of the pores of the support, defect free coating is possible.

The influence of substrate pores on the packing behavior of  $\gamma$ -alumina colloidal particles is clear from the work of Miller et al. [15]. They stated that, in colloidal deposition process, the packing density of the material formed is proportional to the consolidation potential (chemical potential or pressure). Even if the chemical properties and molar volume of the suspension remains the same, the layer density depends on the pore size of the support. In other words, dipping a substrate with a broad pore size distribution or with pinhole like surface irregularities, can lead to a thin layer with local density variations.  $\gamma$ -alumina intermediate layers will, hence, retrace the support surface properties. SEM images of pinholes in such a colloidal layer related to voids in the support surface are shown by Bonekamp et al. [16]. Multi-layered colloidal coatings are sometimes made to minimize these pinholes [3] and subsequent defect formation in the active silica layer.

Despite all these studies, the interaction between the substrate and deposited layer is still not completely known. Sol–gel films can be tailor-made, but substrate selection rules are qualitative. Selectivity to a good extent depends on the quality of the membrane, particularly when the permeability of the slow diffusing component is very small. Permeation through defects will limit selectivity in such situations. Nevertheless, membranes with a high activation energy for small gas molecules can be consistently made using proper sol–gel compositions.

Synthesis of silica membranes showing very high activation energy for helium permeation is presently reported. He/ $N_2$  selectivity also is very high. Permeation of He,  $N_2$  and a number of other molecules are measured. From these results and adsorption studies the pore size of the membrane layer is hypothesized.

## 2. Experimental

Polymeric silica sols were prepared by the acid catalyzed hydrolysis and condensation of tetra-ethyl-ortho-silicate (Wako pure Chemical) in an ethanol medium. Calculated quantities of ethanol and

TEOS were first mixed. Dilute  $\text{HNO}_3$  was then added slowly. The mixture was kept at room temperature for about 30 min. Slow heating was done to raise the temperature of the mixture to  $80^\circ\text{C}$ . The synthesis mixture was made of 1 : 5 : 6.8 : 0.1225 mol% of TEOS : Ethanol : Water :  $\text{HNO}_3$ . After synthesis the mixture was cooled to room temperature and diluted to 0.1 mol with ethanol. Dipping was immediately performed.

Flat supports of alpha alumina ( $12.5\text{ cm}^2$  area) were pressed, sintered and polished. Polishing was carried out in three stages. At first the samples were wet polished (water), followed by polishing with  $2\text{ }\mu\text{m}$  silicon polish and finally with  $0.1\text{ }\mu\text{m}$  diamond slurry. Porosity of this support was 50% and pore size was 150 nm. Infiltration of polishing medium was observed in some of the membranes (measured from weight gain assuming material removal during the final stage polishing as insignificant). These substrates were cleaned in an ultrasonic bath and heat treated at  $800^\circ\text{C}$  after polishing.

These substrates were then dipped into a boehmite sol. Dipping time was 10 s. The synthesis of boehmite sol and procedure of dipping is described elsewhere [3]. On calcination at  $600^\circ\text{C}$  boehmite transformed into gamma alumina.

These membranes were dipped in silica sol for 10 s. Dipping was performed by introducing the support surface tangentially in to the sol kept in flat petri-dish. After the required time the support was withdrawn in the same manner. Drying was performed in a humidity controlled oven at  $40^\circ\text{C}$  and 60% RH. Calcination in air was performed. Samples were heated at  $25^\circ\text{C h}^{-1}$  to  $400^\circ\text{C}$  and soaked for 3 h at that temperature. Unsupported membranes (gel) made from the dip solution were treated in the same way. These gels were used for adsorption studies.

Adsorption was performed on continuous flow equipment (Omnisorp 100 CX) as well as equilibrium adsorption equipment (Bellsorb 28SA). A nitrogen flow rate of  $0.1\text{ ml min}^{-1}$  was used in the continuous flow instrument. In the equilibrium adsorption method (controlled sample dosing depending on manifold pressure variations) low pressure (0–10 Torr) adsorption took approximately one day period. Higher pressures, 10–760 Torr, were recorded faster. Ar adsorption was performed on the first setup.  $\text{N}_2$  adsorption was performed on both setups.

Single gas permeation was carried out on a pressure controlled dead end setup. Gas at constant pressure was introduced in the feed side. Pressure increase in the down stream side was measured. For helium a pressure head of 0–760 Torr and for other gases 0–10 Torr (MKS, Barotron, USA) was used in the down stream side. A testing diameter of 15.8 mm was measured. Leakage was measured as follows. The cell (with membrane) was first heated up and evacuated to remove all adsorbed gases. Leaving the system evacuated, the build up of pressure in the down stream side was measured. (To understand the effect of the O' rings on leakage permeation, an impermeable metal substrate was used in place of the membrane and permeation test was performed). Thus deduced average pressure was used as the correction pressure ( $P_{d2}$ ). Leakage corrected permeation was calculated as follows. Gas permeation  $\propto$  Down stream pressure ( $P_d$ ). Here  $P_d = P_{d1} - P_{d2}$ , where  $P_{d1}$  is the down stream pressure measured during permeation testing and  $P_{d2}$  is the correction pressure value measured during cell leakage test. At low temperatures this pressure increase is very small and can be safely overlooked when the gas permeation is higher than  $10^{-10}\text{ mol m}^{-2}\text{ s}^{-1}\text{ Pa}^{-1}$ . Hence (in case of inorganic membranes) such correction is necessary only when the membranes are of molecular-sieving type exhibiting very low permeation values for specific gases.

### 3. Results and discussion

Nitrogen adsorption studies in continuous flow and equilibrium adsorption equipment gave nearly the same results. Ar and  $\text{N}_2$  (Fig. 1) adsorption results showed a difference in apparent micropore volume. In both cases type 1 [17] adsorption was evidenced. Microporosity of 28% was measured by Ar adsorption and 24% by  $\text{N}_2$  adsorption. The character of sorption isotherms showed the very small pore size of the membrane material. The thickness of the analyzed gel pieces was about 1–2 mm. The supported membrane layers on the other hand were usually smaller than 50 nm [18]. This difference in thickness and the difference in properties of the drying surface were sufficient enough to cause changes in pore size distribution [13]. However our studies have indicated that

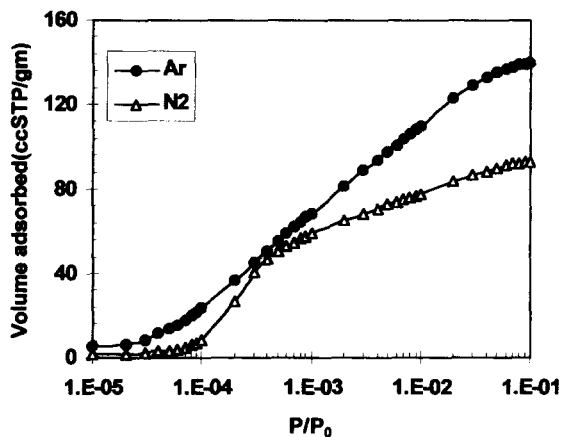


Fig. 1. Ar and N<sub>2</sub> adsorption isotherms of calcined silica gel. The adsorbed volumes correspond to gel microporosity of 28% (Ar) and 24% (N<sub>2</sub>).

a correlation exists between the gel and the supported membrane [19].

Gamma alumina gel was mesoporous. The pore size was 4 nm according to BJ analysis of the N<sub>2</sub> desorption isotherm. The support-gamma alumina layer system showed Knudsen diffusion for helium. Silica coated membranes were microporous. Fig. 2 shows the helium permeation values. Measurement was performed for feed pressures approximating 190, 380, 760 and 1000 Torr. The deviation in the permeation values with pressure was negligible. This was expected since activated diffusion is a pressure inde-

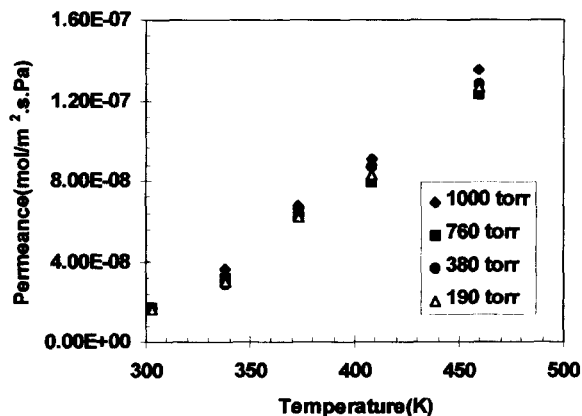


Fig. 2. Helium permeation of microporous silica membrane. Legend is feed pressure in Torr. Permeation was measured by dead end method.

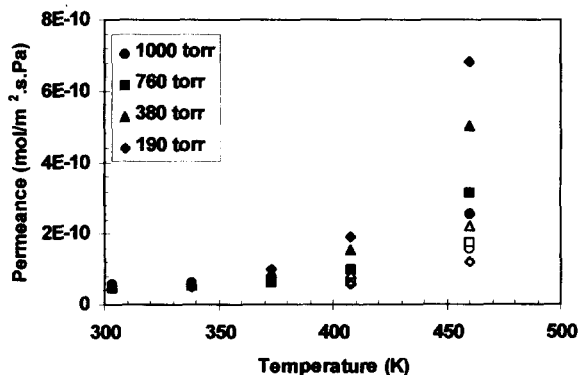


Fig. 3. N<sub>2</sub> permeation of silica membrane. Legend is feed pressure in Torr. Solid symbols correspond to (a) permeation as measured and Open symbols correspond to (b) permeation after subtraction of correction pressure for cell leakage.

pendent process. The contribution from leakage flux was very small because of the relatively high helium permeation value.  $E_{act}$  was calculated as 17 kJ mol<sup>-1</sup> in the temperature range of 303–460 K. This value is uncorrected for support influence. At high temperatures the membrane helium permeability was on the order of 10<sup>-7</sup> mol m<sup>-2</sup> s<sup>-1</sup> Pa<sup>-1</sup> units. The support resistance can be significant for helium [20].

Fig. 3 shows the nitrogen permeation. As in the case of Fig. 2, the points in vertical axis represent the change in permeation with pressure. The variation is insignificant at low temperatures. At high temperatures, particularly at 460 K, the change is significant. The dependence of the measured flux on the leakage flux of the cell could be the reason. The magnitude of this leakage increased sharply around this temperature. The corrected N<sub>2</sub> permeation values also are shown in Fig. 3. The correction process (subtraction of leakage from the measured flux) removed the pressure dependence of N<sub>2</sub> permeation to some extent. The  $E_{act}$  was calculated as 3 kJ mol<sup>-1</sup> from the leakage corrected permeation data.

Helium/nitrogen perm-selectivity is shown in Fig. 4. The reported values are at 1000 Torr feed side pressure. A maximum perm-selectivity of 1236 is available at 408 K. Selectivity drops to 846 at a higher temperature of 460 K. The figure also shows the permselectivity values without correcting for leakage. A maximum value of 922 is available at 408 K. The permselectivity value at 408 K is one of the highest reported; the helium permeation rate of

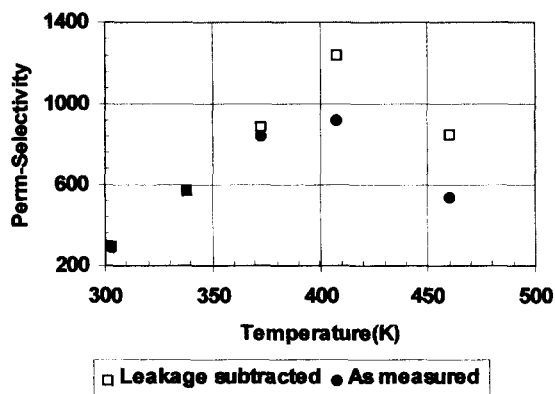


Fig. 4. He/N<sub>2</sub> ideal-selectivity, calculated from single gas permeation results shown in Figs. 2 and 3, at a feed side pressure of 1000 Torr.

$9 \times 10^{-8} \text{ mol m}^{-2} \text{ s}^{-1} \text{ Pa}^{-1}$  at this temperature is reasonable. These high values coupled with the relative ease of synthesis, makes these membranes attractive materials.

Fig. 5 shows the permeation of a number of molecules, other than helium, through the membrane at room temperature. All the measurements were done at 1000 Torr. Permeation of hydrocarbon molecules was larger than that of N<sub>2</sub>, O<sub>2</sub> or Ar. Strong adsorption of the hydrocarbons could be the reason. *n*-Butane showed the highest permeation out of the tested molecules. Further, adsorption experiments revealed that *n*-Butane has the highest adsorption capacity in

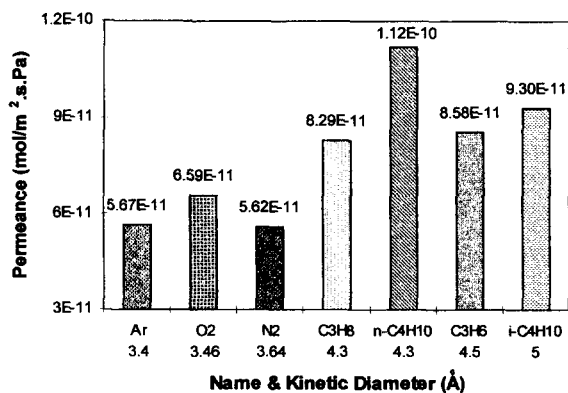


Fig. 5. Permeation of selected gas molecules larger than 3 Å ( $P=1000 \text{ Torr}$ ,  $T=303 \text{ K}$ ). Even though transport was dominated by permeation through defects, the adsorption dependence is notable. Hydrocarbon molecules showed higher permeation values than their inorganic counterparts.

this silica membrane material. None of the gas molecules shown in Fig. 5, showed significant  $E_{\text{act}}$  for diffusion in the temperature range of 303–408 K. This coupled with the low permeation values, indicates that most of the permeation is through defects (non-selective) in the membrane.

The results so far discussed point to the characteristic pore size distribution of the active layer. The apparent activation energy of  $17 \text{ kJ mol}^{-1}$  (uncorrected) reported for helium is a convincing proof of the involvement of extremely small pore sizes. The activation energy of N<sub>2</sub> is very small. Non-activated flux dominated N<sub>2</sub> permeation. Hence the defects in the membrane were the prominent transport path for N<sub>2</sub> molecules. In other words, the majority micropore volume acted dense (insignificant permeation rate) for N<sub>2</sub> permeation. This may be the case for all tested gases other than helium and hydrogen. Hydrogen permeation was slightly higher than helium permeation. For a (similar) membrane with room temperature helium permeation of  $4 \times 10^{-9} \text{ mol m}^{-2} \text{ s}^{-1} \text{ Pa}^{-1}$  at 4 bar feed side pressure, hydrogen permeation was measured as  $4.5 \times 10^{-9} \text{ mol m}^{-2} \text{ s}^{-1} \text{ Pa}^{-1}$  under identical conditions. This shows a H<sub>2</sub>/He selectivity of 1.12 at room temperature. This trend of higher H<sub>2</sub> permeation is similar to other reported silica membranes [20] and highlights the potential of this membrane for H<sub>2</sub> separation applications such as membrane reactors for dehydrogenation reactions.

As already stated the permeation rate of all gas molecules other than helium and hydrogen was insignificant, indicating a majority pore size in the 3 Å region. This is in contrast to other reported silica membranes [1,3,13]. A bi-modal micropore size distribution with 5 Å and a sizable proportion of 7–8 Å pores was commonly seen. The absence of this tail of larger pores in the present membrane could be the reason for the high selectivity (He/N<sub>2</sub>) and high helium apparent activation energy.

The reason for the absence of larger pores in the present sample can not be explained fully at this stage. The porosity in silica membranes was formed by two causes; owing to the intrinsic nature of the fractal aggregates and from the collapse of the adsorbed gel layer on drying [12]. These different mechanisms essentially force the membrane to have two different pore sizes. The first factor depends only on synthesis history and the second on synthesis as well as drying

Table 1

Comparison of the characteristics of three silica samples with identical processing history.  $E_{\text{act}}$  for helium permeation is consistently high irrespective of the changes in defect concentration

Sample	Microporosity (%)	He perm at 408 K (mol m <sup>-2</sup> s <sup>-1</sup> Pa <sup>-1</sup> )	He $E_{\text{act}}$ (kJ mol <sup>-1</sup> )	N <sub>2</sub> perm at 408 K (mol m <sup>-2</sup> s <sup>-1</sup> Pa <sup>-1</sup> )	He/N <sub>2</sub> at 408 K
1	23.93	3.58E-08	19.6	7.37E-11	485.11
2	—	4.06E-08	22.5	1.28E-10	316.31
3	24.81	8.59E-08	19.2	1.28E-09	66.63

rate and support constraints. It is difficult to conclude the relative importance of the parameters. It is realized that synthesis changes can bring large changes in the permeation and activation energy even under same support processing conditions. As an example, an increase of 25% of the molar amounts of H<sub>2</sub>O and HNO<sub>3</sub> (from the present composition) leads to a membrane with helium activation energy of 7.98 kJ mol<sup>-1</sup> [19]. This suggests that the present selection of synthesis composition and variables lead to similar intrinsic and collapsed pore sizes to a good extent.

Our own past results have indicated [18] that sol-gel synthesis under milder reaction conditions leading to membranes with lesser activation energy of 9.3 kJ mol<sup>-1</sup>. Such conditions should lead to close packing of polymers leading to denser membranes. Unsupported membranes of course showed this trend with a lower porosity of 20% compared to 24% in the present case. But the helium permeation was about 3 times higher than the present membranes showing the presence of defects in the membrane. One reason for the poor performance should be the inferior support surface quality. Even under the present support conditions inconsistency in performance was observed between membranes as follows.

The characteristics of three membranes with identical processing history is shown in Table 1. Synthesis composition and conditions, drying, sintering, etc., were the same. As can be seen, in the case of unsupported gels the difference in microporosity between the samples was insignificant. Helium activation energies (from 303–373 K permeation data to keep support influence minimum) of all the membranes were almost the same. The N<sub>2</sub> permeation of membrane number 3 was seemingly different from the others. The same trend is reflected in the He/N<sub>2</sub> selectivity.

The similar values of  $E_{\text{act}}$  show that the active layer pore structures of all the three membranes were almost identical. Obviously sample 3 had more defects in the testing area. Non-activated N<sub>2</sub> flux through the membrane was high, reducing the permselectivity. Gel microporosity being the same, the leakage pores might have been produced during the dipping and/or drying stage. It can be assumed that defects in varying degrees and concentrations, even though insignificant, are formed across the membrane even under the present support processing conditions.

The results so far discussed have revealed some significant clues on the most important processing parameters deciding the final membrane behavior. Earlier works [10] have established the significance of controlling synthesis compositions and environment on deciding the final pore structure of unsupported gels. The fractal dimension of the silica polymers and the porosity of the gel are found to vary in a systematic way. Ways to tailor make silica microporous unsupported membranes were discussed. It was expected that this set of rules would also govern the formation of supported membranes. However the present investigation has revealed the relative importance of supports in deciding the defect concentration and hence selectivity. Nevertheless activation energy for helium diffusion can be consistently reproduced under the same support conditions.

#### 4. Conclusions

1. Microporous membranes with He/N<sub>2</sub> perm-selectivity of 1236 at 408 K can be prepared by sol-gel modification techniques.

2. The permeation through the membrane was mainly selective diffusion through ultra-micropores (3 Å) of the membrane, but non-selective diffusion

through the defects was evident in the case of molecules bigger than 3 Å.

3. Apparent activation energy for helium permeation was consistently high, irrespective of the fact that defect concentration varied among membranes of identical processing history.

### Acknowledgements

A part of this work has been conducted by the support of the Petroleum Energy Center (PEC) subsidized from the Ministry of International Trade and Industry, Japan. We also acknowledge the help of Ms. Momoyo Aizawa and Ms. Keisuke Sato of JHPC and Mr. Takashi Sugawara and Mrs. Keiko A. Koyano, of the University of Tokyo for experimental assistance.

### References

- [1] C.J. Brinker, T.L. Ward, R. Sehgal, N.K. Raman, S.L. Hietala, D.M. Smith, D.-W. Hua and T.J. Headley, Ultra-microporous Silica-based Supported Inorganic Membranes, *J. Membr. Sci.*, 77 (1993) 165.
- [2] A. Julbe, C. Guizard, A. Larbot, L. Cot and A. Giroir-Frendler, The Sol–Gel Approach to Prepare Candidate Microporous Inorganic Membranes for Membrane Reactors, *J. Membr. Sci.*, 77 (1993) 137.
- [3] R.J.R. Uhlhorn, K. Keizer and A.J. Burggraaf, Gas Transport and Separation with Ceramic Membrane. Part I and II, *J. Membr. Sci.*, 66 (1992) 259, 271.
- [4] S. Kitao, H. Kameda and M. Asaeda, Gas Separation by Thin Porous Silica Membrane of Ultra Fine Pores at High Temperature, *Membrane*, 15(4) (1990) 222.
- [5] R.S.A. de Lange, J.H.A. Hekkink, K. Keizer and A.J. Burggraaf, Preparation and Characterization of Microporous Sol–Gel Derived Ceramic Membranes for Gas Separation Applications, *Mat. Res. Soc. Symp. Proc.*, 271 (1992) 505.
- [6] M. Tsapatsis and G. Gavalas, Structure and Aging Characteristics of H<sub>2</sub> Permselective SiO<sub>2</sub> Vycor Membranes, *J. Membr. Sci.*, 87 (1994) 281.
- [7] S. Yan, H. Maeda, K. Kusakabe, S. Morooka and Y. Akiyama, Hydrogen Permselective SiO<sub>2</sub> Membrane Formed in Pores of Alumina Support Tube by Chemical Vapor Deposition with Tetraethyl Ortho Silicate, *I & EC Research.*, 33 (1994) 2096.
- [8] J.C.S. Wu, H. Sabol, G.W. Smith, D.L. Flowers and P.K.T. Liu, Characterization of Hydrogen Permselective Microporous Ceramic Membranes, *J. Membr. Sci.*, 96 (1994) 275.
- [9] L.C. Klein, Sol–Gel Processing of Silicates, *Ann. Rev. Mater. Sci.*, 15 (1985) 227.
- [10] J.W. Elferink, B.N. Nair, R.M. de Vos, K. Keizer and H. Verweij, Sol–Gel Synthesis and Characterization of Microporous Silica Membranes, *J. Colloid and Interface Sci.*, 180 (1996) 127.
- [11] C.J. Brinker and G.W. Scherer, Sol–Gel Science: The Physics and Chemistry of Sol–Gel Processing, Academic Press, London (1990).
- [12] C.J. Brinker, N.K. Raman, M.N. Logan, R. Segal, R.-A. Assink, D.-W. Hua and T.L. Ward, Structure Property Relationships in Thin Films and Membranes. *J. Sol–Gel Sci. Tech.*, 4 (1995) 117.
- [13] R.S.A. de Lange, K. Keizer and A.J. Burggraaf, Analysis and Theory of Gas Transport in Microporous Sol–Gel Derived Ceramic Membranes, *J. Membr. Sci.*, 104 (1995) 81.
- [14] M. Moaddeb and W.J. Koros, Silica-Treated Ceramic Substrates for Formation of Polymer–Ceramic Composite Membranes, *Ind. Eng. Chem. Res.*, 34 (1995) 263.
- [15] K.T. Miller, R.M. Melant and C.F. Zukoski, Comparison of the Compressive Yield Response of Aggregated Suspensions: Pressure Filtration, Centrifugation, and Osmotic Consolidation. *J. Amer. Ceram. Soc.* (1996), in press.
- [16] B.C. Bonekamp, Preparation of asymmetric ceramic membrane supports by dip-coating, In A.J. Burggraaf and L. Cot (eds.), *Fundamentals of Inorganic Membrane Science and Technology*, Elsevier, Amsterdam (1996) 141.
- [17] S.J. Gregg and K.S.W. Sing, Adsorption Surface Area and Porosity, Academic Press, London (1982).
- [18] B.N. Nair, K. Keizer, J.W. Elferink, M.J. Gilde, H. Verweij and A.J. Burggraaf, Synthesis, Characterization and Gas Permeation Studies on Microporous Silica and Alumina–Silica Membranes for Separation of Propane and Propylene, *J. Membr. Sci.*, 116 (1996) 161.
- [19] B.N. Nair, K. Keizer, T. Okubo and S.I. Nakao, Evolution of Pores in Molecular Sieving Silica Membranes: Sol–gel Procedures and Strategies., to be Communicated to *Ind. Engg. Chem. Res.* (1997).
- [20] R.S.A. de Lange, Microporous Sol–Gel Derived Ceramic Membranes for Gas Separation., Ph.D. thesis, University of Twente, The Netherlands (1993).